SAGE-Hindawi Access to Research
Journal of Tissue Engineering
Volume 2011, Article ID 615328, 9 pages
doi:10.4061/2011/615328

Research Article

The Chemical and Physical Properties of Poly(ε-caprolactone) Scaffolds Functionalised with Poly(vinyl phosphonic acid-co-acrylic acid)

A. K. Bassi, J. E. Gough, M. Zakikhani, and S. Downes

School of Materials, The University of Manchester, Grosvenor Street, Manchester M1 7HS, UK

Correspondence should be addressed to S. Downes, sandra.downes@manchester.ac.uk

Received 25 May 2011; Revised 25 August 2011; Accepted 26 August 2011

Academic Editor: Wojciech Chrzanowski

There is a clinical need for a synthetic alternative to bone graft substitute (BGS) derived from demineralised bone matrix. We report the electrospinning of Poly(ε-caprolactone) (PCL) to form a 3-dimensional scaffold for use as a synthetic BGS. Additionally, we have used Poly(vinyl phosphonic acid-co-acrylic acid) (PVPA) to improve bone formation. Fibres were formed using a 10% w/v PCL/acetone solution. Infrared spectroscopy confirmed that the electrospinning process had no effect on the functional groups present in the resulting structure. The electrospun scaffolds were coated with PVPA (PCL/PVPA), and characterised. The stability of the PVPA coating after immersion in culture medium was assessed over 21 days. There was rapid release of the coating until day 2, after which the coating became stable. The wettability of the PCL scaffolds improved significantly, from 123.3 ± 10.8° to 43.3 ± 1.2° after functionalisation with PVPA. The compressive strength of the PCL/PVPA scaffolds (72 MPa) was significantly higher to that of the PCL scaffold (14 MPa), and an intermediate between trabecular and cortical bone (7 MPa and 170 MPa, resp.). The study has demonstrated that the PCL/PVPA scaffold has the desired chemical and biomechanical characteristics required for a material designed to be used as a BGS.

1. Introduction

There is a need for a synthetic bone graft substitute with active properties capable of stimulating bone tissue regeneration. In the past, research has focused on the development of bioinert materials [1, 2], materials that have no effect on the surrounding tissue. More recently, focus has shifted to bioactive materials, which interact with the surrounding tissue and encourage bone regeneration and osteointegration [3]. There are a number of synthetic bone graft substitutes available; however, none have been found to match or better the properties associated with autografts and demineralised bone matrix (DBM). The ideal bone graft substitute must have certain characteristics and properties in order for effective bone formation to occur (Table 1).

The morphology of scaffolds for bone tissue engineering has a large influence on the cell response. Research has been directed to matching the properties of tissue on the macroscopic level; however, cells have been found to respond to the fibrous, nanoscale structure of the extracellular matrix (ECM) [4]. The natural ECM of bone is composed of collagen fibres embedded in a matrix of proteoglycans. Bone cells interact with this matrix, and ideally a scaffold that mimics this morphology of the ECM may aid in optimising the properties of scaffolds to improve bone formation.

Over the last decade, electrospinning has become an emerging field to produce scaffolds for bone tissue engineering. Electrospinning is a process by which fibres can be produced through an electrically charged jet of polymer solution. A range of materials, from natural polymers to synthetic polymers have been successfully electrospun into porous scaffolds for use in tissue engineering. The use of calcium apatites and hydroxyapatite is another approach in improving bone formation. The ECM of bone, consists of an inorganic hydroxyapatite phase, therefore the incorporation of hydroxyapatite into an electrospun, fibrous scaffold could provide biomimicry. Li et al. [5] and Venugopal et al. [6] are just two research groups of many that have incorporated

Table 1: The desirable properties required for a bone tissue engineered scaffold for successful bone regeneration [12–16].

Desirable properties	Advantages
Biocompatible	(i) Nonimmunogenic (ii) Nontoxic
Porosity	(i) Ideal porosity ≈ 90% (ii) Allows the infiltration of cells and nutrients (iii) Removal of waste products (iv) Greater surface area for cell attachment and proliferation
Biodegradable	(i) Temporary structure for the attachment and proliferation of cells (ii) Degrades as new bone is deposited (iii) Eliminating the need for further invasive surgery (iv) Degradation products are non toxic and easily secreted through metabolic pathways
Osteoconductive	(i) Support bone growth and encourage ingrowth of surrounding bone
Osteoinductive	(i) Induces the differentiation of stem cells into mature osteoblasts
Mechanical properties	(i) Stable for surgical handling (ii) Able to withstand the forces exerted by the body

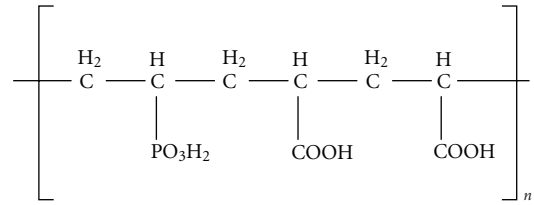

Figure 1: The chemical structure of poly(vinyl phosphonic acid-co-acrylic acid). The close proximity of the P-C groups with other molecules mimics the P-C–P backbone found in bisphosphonates.

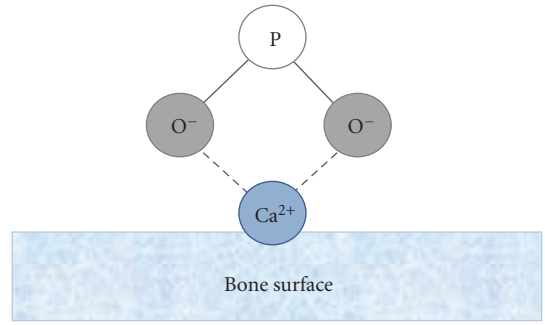

Figure 2: The PO_3H_2 group present in PVPA is hypothesised to chelate Ca^{2+} ions by forming a "bone hook," which will lead to an increase in mineralisation.

hydroxyapatite into a polymeric scaffold. Although this approach has been found to improve matrix formation, there are problems associated with the dissolution of hydroxyapatite and poor healing of more challenging defects or bone that is associated with low density, such as osteoporosis and Paget's disease.

We have identified a phosphonate-containing polymer, poly(vinyl phosphonic acid-co-acrylic acid) (PVPA) (Figure 1) [7] which is hypothesised to mimic the action of bisphosphonates, a group of drugs used in the treatment of osteoporosis [8]. The close proximity of P-C groups within the structure are speculated to mimic the P-C-P backbone found in bisphosphonates which act by inducing osteoclast apoptosis leading to an increase in bone formation [9–11]. The close proximity of the P-C groups coupled with the strong negative charge of the ions, the PVPA polymer is hypothesised to chelate calcium ions (Figure 2). Phosphonic acid containing polymers have also been described to improve mineralisation in a dose-dependent manner, therefore promoting osteoblast maturation.

Recently, researchers have attempted to incorporate bisphosphonates within substrates such as hydroxyapatite and demonstrated osteoclast apoptosis; however, these composite systems fail to provide the mechanical support required in load-bearing applications [17, 18]. The modification of polymer substrates with bisphosphonates has been investigated, and although the mechanical strength of the scaffold may improve, the well-documented side effects of bisphosphonates may still occur [19]. A polymeric substitute could offer a solution to these problems.

In this study electrospinning has been used to fabricate a scaffold composed of Poly(ε-caprolactone) and Poly(vinyl phosphonic acid-co-acrylic acid) (hereafter referred to as PCL/PVPA) for use as a synthetic bone graft substitute. The fibrous nature of the scaffold resembles the collagen fibres found in the extracellular matrix of bone thus providing a biomimetic structure for cell attachment and proliferation. The combined positive effects of the PVPA polymer on the osteoblast and osteoclast cell are hypothesised to lead to a net increase in bone formation. The aim of the present study is to describe the fabrication process and evaluate the physical and biomechanical properties of the novel polymer system and to describe the preliminary results obtained from *in vitro* cell culture using osteoblast and osteoclast cells.

2. Materials and Methods

2.1. Fabrication of PCL Fibres

2.1.1. Electrospinning. A 10% w/v polymer solution of PCL ($M_n \approx 80,000$) in acetone was electrospun using an applied voltage 20 kV, flow rate 0.05 mL/min, and a needle collector

distance 15 cm. Fibres were collected on a grounded collector plate to give a randomly orientated morphology.

2.1.2. Preparation of PCL/PVPA Films. Films of PCL/PVPA were prepared by immersing the electrospun PCL mat in a reservoir of 15% PVPA in deionised water for 24 hours. The films were removed from the PVPA and formed into a 3D spherical scaffold. The scaffolds were air dried for 48 hours and then heat-treated at 55°C for 24 hours.

2.2. Characterisation of Polymer Scaffolds

2.2.1. Morphology of Scaffolds. Scaffolds were mounted onto aluminium stubs using carbon tabs (Agar Scientific, UK) and then carbon coated using the Edwards E306A Coating System. The coated scaffolds were viewed in a Phillips XL30 Field Emission Gun Scanning Electron microscope (FEG-SEM, Phillips XL30) using an accelerating voltage of 5 kV, a spot size of 3, and a working distance of 10 mm. The average fibre diameter was calculated by measuring the diameter of 100 fibres using Image J software (National Institutes of Health, USA).

2.2.2. Phosphorous Concentration. The concentration of phosphorous within the scaffolds was monitored using energy dispersive X-ray spectroscopy (EDX) after drying the scaffolds upon immersion in Dulbecco's Modified Eagle Medium (DMEM) for a total of 21 days. At days 2, 7, 14, and 21, scaffolds were removed from the DMEM, washed with deionised water, and air dried for 24 hours.

Scaffolds were mounted and carbon coated using the Edwards E306A Coating System. The coated scaffolds were viewed in a Phillips XL30 Field Emission Gun Scanning Electron microscope (FEG-SEM, Phillips XL30) using an accelerating voltage of 5 kV and a working distance of 10 mm. The FEG-SEM has an EDX spectrometer, which detects the released X-rays from the scaffold. EDX analysis was carried on PCL/PVPA scaffolds that had undergone heat treatment and unheated scaffolds in triplicate.

2.2.3. Wettability of Scaffolds. The contact angle of the scaffolds was tested using the Krüss DSA 100 Drop Size Analyser. The wettability of electrospun PCL, and electrospun PCL/PVPA was tested on three randomly selected scaffolds. A 10 μL droplet of distilled water was released onto each scaffold using an 8-gauge needle (BD Plastics, UK), the change in contact angle was measured over 7.20 seconds.

2.2.4. Determination of Functional Groups. Fourier Transform Infrared Spectroscopy (FTIR) spectra were collected using the Thermo Nicolet Nexus FTIR (Cambridge, UK). Scaffolds were mounted on to the smart orbit sampler, which was connected to the FTIR Nexus. OMNIC software was used for the analysis of the collected spectra. Spectra's were obtained by accumulating 32 scans in the range of 400–4000 cm^{-1} with a resolution of 4 cm^{-1}. The data is expressed as the average of 3 spectra for each scaffold.

2.2.5. Thermal Properties of Polymer Scaffolds. Differential scanning calorimetry (DSC, Q100 V9.8) was used to determine the thermal properties of the various polymer films. Scaffolds were sealed hermetically in aluminium pans and heated within the range of −90°C to 150°C with a heating rate of 10°C/min. The nitrogen gas flow rate was 50 mL/min and measurements were carried out at a scanning rate of 10°C/min using a heat/cool/heat cycle. The repeated heating and cooling removes any thermal history. An empty reference pan was used to subtract the blank so that only the thermal properties of the material were detected.

2.2.6. Mechanical Properties of Polymer Scaffolds. The compressive strength and Young's modulus of the scaffolds were determined using the Instron 1122 mechanical tester at a temperature of 23 ± 1°C and relative humidity of 50 ± 2%. A compression plate attachment was used for the test. A crosshead speed of 50 mm/min was used and the distance between the two plates was 11 mm. The full-scale load was set at 0.20 kN.

2.3. Assessment of Biocompatibility

2.3.1. Osteoblast Culture. Human osteoblast cells (HOBs) (The European Collection of Cell Cultures, UK; cell line no. 406-05a) were cultured in Dulbecco's modified Eagles medium (DMEM; Gibco, Paisley) supplemented with 10% FBS, antibiotics (100 U/mL penicillin, 100 mg/mL streptomycin) and 50 μM ascorbic acid. Culture medium was replenished every 2 days. Scaffolds were immobilised in 24-well plates using Cell Crown inserts (Scaffdex, Finland) and sterilised using a series of increasing ethanol concentrations. Cells were counted and seeded onto scaffolds at a density of 40,000 cells/cm^2. Plates were cultured under standard conditions, at 37°C with 95% humidity and 5% CO_2.

At day 14, cells were fixed with 3% paraformaldehyde and stained using Alexa Fluor 488 phalloidin and DAPI Prolong (Invitrogen, UK).

2.3.2. Osteoclast Culture. Human osteoclast precursor cells (Lonza, UK) were dispersed in osteoclast precursor basal medium (α-MEM) supplemented with 10% FBS, 66 ng/mL RANK-L, 33 ng/mL M-CSF, antibiotics (100 U/mL penicillin, 100 μg/mL streptomycin), and 2 mM L-glutamine (all supplied by Lonza, UK). Scaffolds were sterilised and prepared as described in Section 2.3.1 Cells were counted and seeded onto scaffolds and glass cover slips (Agar Scientific, UK) at a density of 60,000 cells/cm^2. Plates were cultured under standard conditions, at 37°C with 95% humidity and 5% CO_2.

At days 1 and 7, cells were washed with PBS and fixed in 1.5% glutaraldehyde in PBS for 30 minutes at 4°C. The scaffolds were then dehydrated through a series of increasing concentrations of ethanol. Samples were dried using hexamethyldisilazane (HMDS). Samples were carbon coated using the Edwards E306A Coating System and viewed

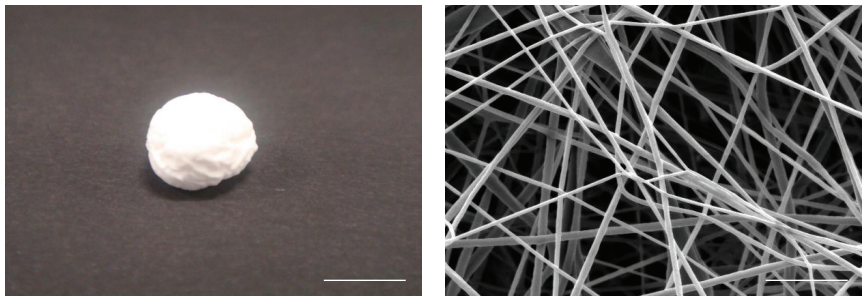

(a) (b)

Figure 3: (a) Photograph of PCL/PVPA 3D scaffold, scale bar 1 cm (b) SEM micrograph of PCL fibres treated with PVPA, fibres had an average diameter of 269 ± 102 nm. Scale bar 5 μm.

in a Phillips XL30 Field Emission Gun Scanning Electron microscope (FEG-SEM, Phillips XL30) using an accelerating voltage of 5 kV and a spot size of 3.

2.4. Statistical Analysis. Statistical evaluation of data was performed using GraphPad software package. Data are reported as mean ± standard deviation (SD) at a significance level of $P < 0.05$. One-way ANOVA with the Bonferroni test was carried out to compare the groups.

3. Results and Discussion

The design of a synthetic bone graft substitute for load-bearing applications requires consideration of the chemical, biomechanical, and biological properties. Here we describe the fabrication, and characterisation of a 3D electrospun scaffold and its potential use as a bone graft substitute.

3.1. Materials Characterisation. Electrospun fibres closely mimic the extracellular matrix of bone [21–23], the fibres obtained during this study had an average diameter of 269 ± 102 nm with most fibres distributed between 100 and 300 nm (Figure 3).

The stability of the PVPA coating was examined using EDX analysis (Figure 4). The presence of phosphorous was monitored over a 21-day period after immersion of the scaffolds in DMEM. Scaffolds that had not undergone heat treatment were tested as a control. There was a sharp decrease in phosphorous wt% from day 0 to day 2 on both scaffold types, decreasing from 3.3 ± 0.08 wt% to 1.24 ± 0.13 wt% on heat-treated scaffolds and to 0.12 ± 0.02 wt% on untreated scaffolds. The initial release of phosphorous in the first two days of immersion could be advantageous *in vivo* as the apoptosis of osteoclasts immediately after implantation would allow osteoblasts to secrete matrix.

After day 2, there was no significant change in phosphorous concentration over the remaining culture period as shown in Figure 5; however, there was a significant difference in concentration between the two scaffold types; scaffolds which had undergone a heat treatment had a significantly higher ($P < 0.001$) concentration of phosphorous compared to untreated scaffolds. This result suggests that after the initial dissolution of PVPA, the coating becomes stable upon heat treatment.

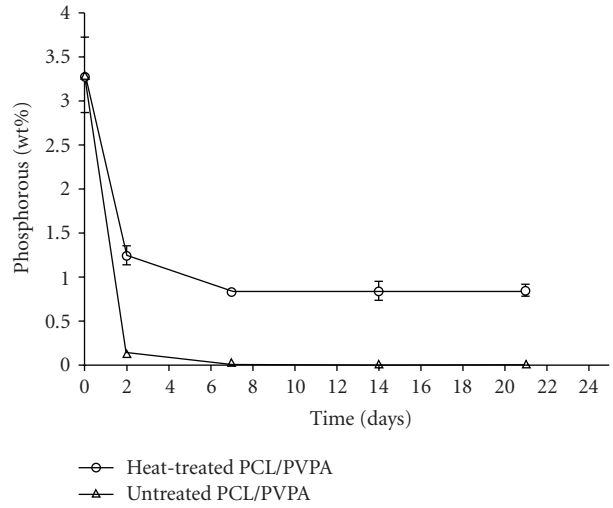

Figure 4: The phosphorous concentration on the surface of the polymeric scaffolds examined through EDX over 21 days ($n = 4$).

It is hypothesised that PVPA is bound to PCL at the interface as a monomolecular layer, and there are subsequent interactions between the unbound PVPA molecules. It is suggested that up till day 2, the unbound PVPA are gradually released. This is followed by stabilisation of the coating as all unbound PVPA are released and only the monolayer of PVPA exists on the surface.

EDX revealed that the heat treatment of PCL/PVPA prevents the PVPA from being removed from the scaffold. During heat treatment the scaffold is taken above its crystallisation temperature. This leads to movement of the polymer chains and cooling leads to subsequent crystallisation of the polymer chains. The PVPA could become "trapped" during the heating and cooling of the polymer chains, which subsequently provides a stable PCL/PVPA scaffold.

The wettability of PCL/PVPA and PCL scaffolds was determined through water contact angle testing (Figure 5). There is a significant difference in the contact angle of PCL scaffolds once treated with PVPA, the contact angle is

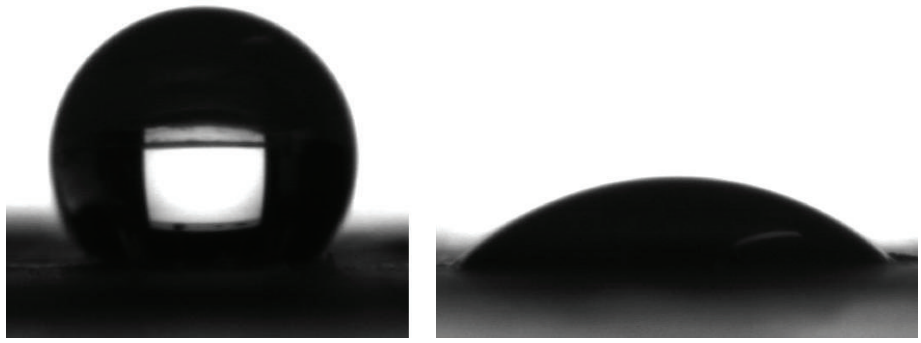

(a) (b)

Figure 5: Photograph images of 10 μL water droplet on (a) PCL scaffold, (b) PCL/PVPA scaffold ($n = 3$).

Table 2: Water contact angle of PCL and PCL/PVPA scaffolds ($n = 3$).

Material	Contact angle
Electrospun PCL	123.3 ± 10.8°
PCL/PVPA	43.3 ± 1.2°

reduced from 123.3 ± 10.8° to 43.3 ± 1.0° (Table 2). The use of PCL without any pretreatment can be limited due to the hydrophobic nature of the polymer. The wettability testing demonstrates that the treatment of PCL with PVPA significantly improves the wetting nature of the polymer and no further treatment would be needed before cell seeding.

PVPA consists of negatively charged –COOH and –OH functional groups. The oxygen atoms exert a greater "pull" on the hydrogen atoms and consequently one of the atoms become electronegative. These groups are said to be polar and are therefore attracted to water as water is also polar, this property will make PVPA hydrophilic and consequently when PCL is treated with PVPA, the surface becomes hydrophilic.

FTIR analysis was employed to identify any changes in the chemical structure that could have occurred during the electrospinning process. When we compare electrospun PCL and a PCL pellet, the spectra reveals that there is no difference in the functional groups present after-electrospinning (Figure 6(a)). The change in the spectra upon the addition of PVPA to PCL reveals a –OH peak at 3450 cm^{-1} (Figure 6(b)). This peak can be owed to the PVPA polymer, which contains many –OH functional groups. The C–H peaks present at 1750 cm^{-1} and 2850 cm^{-1} in electrospun PCL remained unchanged in the presence of PVPA. FTIR analysis has demonstrated that the electrospinning process has no effect on the functional groups present in the resulting structure.

The thermal properties of the polymer scaffolds were determined through DSC; the results are outlined in Table 3. The treatment of PCL with PVPA has had no significant difference on the thermal properties of the scaffolds. This is most likely due to there being only a low concentration of PVPA in comparison to the PCL substrate therefore having no significant effect on the thermal properties.

Table 3: The melting temperature, crystallisation temperature and glass transition temperature of PCL and PCL/PVPA scaffolds ($n = 3$).

Material	Melting temperature (T_m) (°C)	Crystallisation temperature (T_c) (°C)	Glass transition temperature (T_g) (°C)
PCL scaffold	56.53 ± 1.42	26.94 ± 1.76	−59.22 ± 2.79
PCL/PVPA scaffold	56.79 ± 2.75	27.74 ± 1.23	−59.88 ± 1.68

Table 4: Biomechanical properties associated with PCL, PCL/PVPA scaffolds, cortical bone, and trabecular bone* [20].

Material	Compressive strength (MPa)	Young's modulus (GPa)
PCL scaffold	14 ± 1.2	0.9 ± 0.1
PCL/PVPA scaffold	72 ± 4.9	3.9 ± 0.9
Cortical bone*	170–193	14–20
Trabecular bone*	7–10	0.05–0.5

The mechanical properties of a material to be used in bone tissue engineering have an important role in the scaffold design. Mechanical testing was carried out to determine the compressive strength and Young's modulus of the polymer scaffolds. The two properties were determined using previously reported equations and the load-displacement curve obtained (Figure 7). The load-displacement curve displays a significant difference between the load withstood by PCL and PCL/PVPA. The compressive strength of PCL/PVPA scaffolds has been calculated to be 72 MPa, this is significantly higher than that of PCL scaffolds (14 MPa) (Table 4). A similar trend was determined for the Young's modulus, the Young's modulus of PCL/PVPA was determined to be 3.9 GPa and 0.9 GPa for PCL scaffolds. The compressive strength of PCL/PVPA is ten-times greater than that of

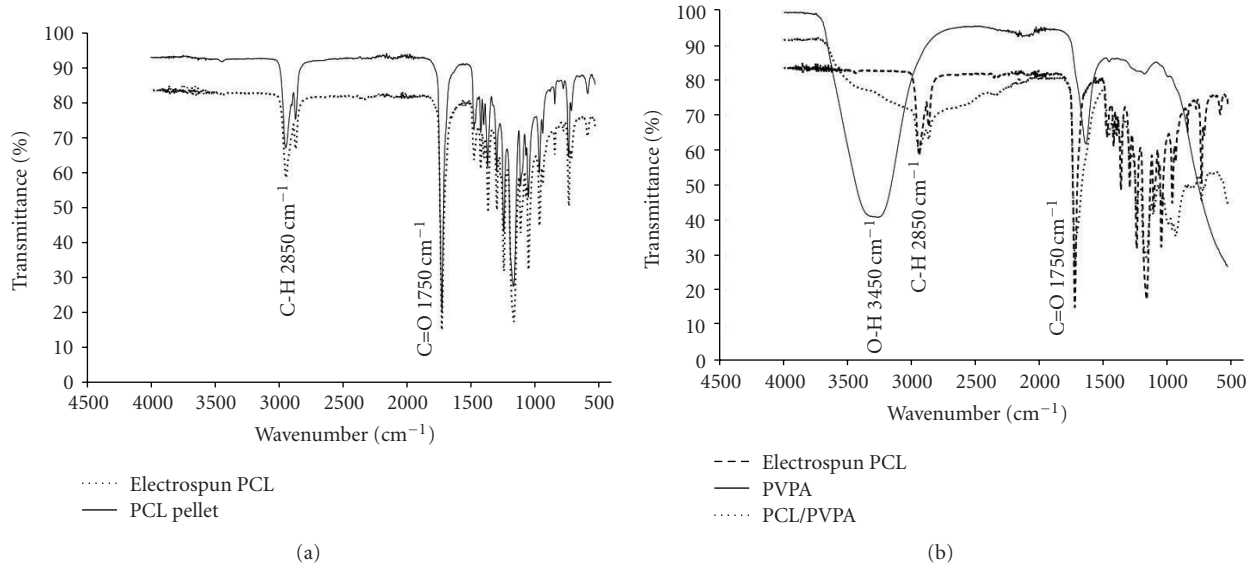

Figure 6: (a) FTIR spectra for a PCL pellet and electrospun PCL. (b) FTIR spectra for PVPA, PCL/PVPA, and electrospun PCL.

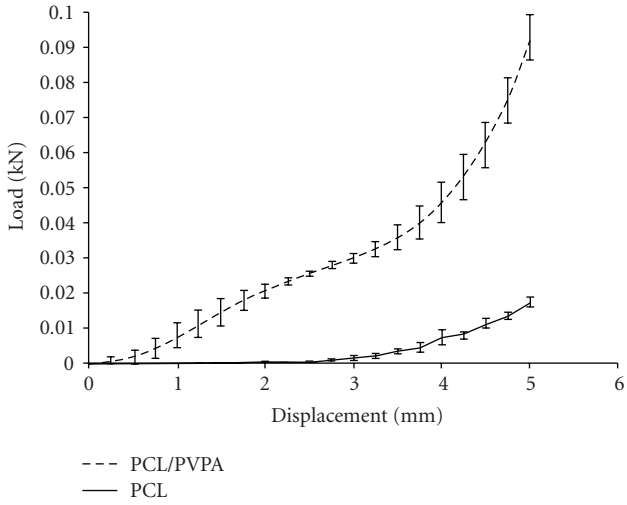

Figure 7: A load-displacement curve showing the loading pattern up to 50% compression of PCL and PCL/PVPA scaffolds ($n = 5$).

trabecular bone (7–10 MPa), and the Young's modulus is eight times greater (0.05–0.5 GPa).

The significant increase in mechanical strength in the presence of PVPA could be owed to the presence of intermolecular interactions between the PVPA-coated PCL scaffolds. The highly negatively charged oxygen atoms within PVPA are attracted to hydrogen atoms present within the scaffolds structure, this interaction provides strength to the resulting structure and hence an increase in the compressive strength.

In the area of bone tissue engineering it is important to closely mimic the natural strength of bone as possible. This can be problematic due to the high compressive strength of bone. The mismatch of mechanical properties between natural bone and synthetic materials can lead to failure of an implanted material. The mechanical properties suggest that the scaffolds have sufficient mechanical strength to be used as a packing substance in trabecular bone voids. The increase in the mechanical properties of PCL/PVPA scaffolds is owed to the properties of PVPA. The solidification of PVPA gives rise to a strong material that is hypothesised to be stronger than PCL. The tensile and compressive properties of PVPA have not been tested. It is hypothesised that the presence of PVPA throughout the PCL structure would provide strength throughout the structure and hence sufficient mechanical support in bone tissue. The mechanical properties of the scaffold can be tailored by changing the amount of PVPA present within the structure. An optimum concentration will have to be determined to allow for an advantageous effect on cells growth as well as on the mechanical properties.

3.2. Biocompatibility. Preliminary studies have shown that osteoblast cells are able to favourably attach and proliferate on the PCL/PVPA scaffold (Figure 8). After 14 days in culture, a more pronounced cytoskeleton was observed in osteoblasts cultured on PCL/PVPA scaffolds, this is most likely to be due to superior spreading of the cells due to the significantly lower water contact angle of the PCL/PVPA scaffold when compared to PCL scaffolds [23, 24]. Further studies investigating the effects of the scaffold on osteoblast activity will be carried out.

Scanning electron microscopy (SEM) was used to visualise osteoclasts cultured on PCL, PCL/PVPA, and glass substrates over 7 days under standard conditions. At day 1, there were viable cells present on all scaffold types (Figure 9). A high number of cell colonies formed on PCL/PVPA scaffolds. It is not clear whether this is due to the hydrophilic nature of the substrate which encourages rapid attachment of cells or whether it is due to the PVPA polymer causing cells to group together and a possible indicator of the initiation of apoptosis. Cells present on both PCL and PCL/PVPA

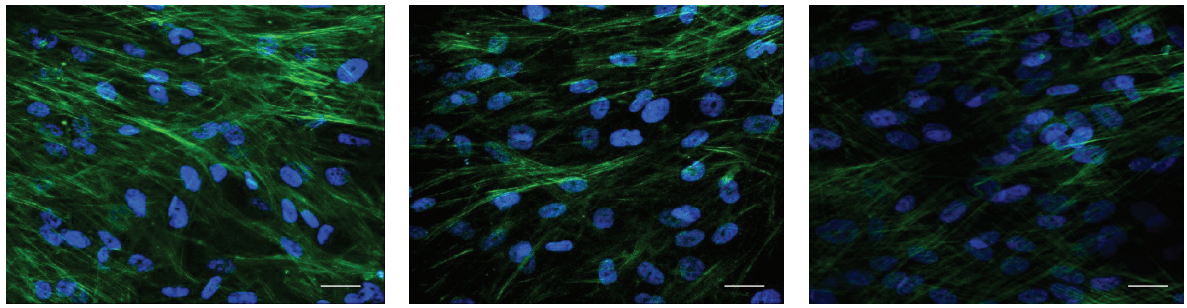

(a) (b) (c)

Figure 8: Fluorescence micrograph images of human osteoblast cells cultured for 14 days on (a) PCL/PVPA, (b) PCL, and (c) Tissue culture plastic. Staining of nuclei (DAPI, blue) and cytoskeleton (Alexa Fluor 488 phalloidin, green). Scale bar 25 μm.

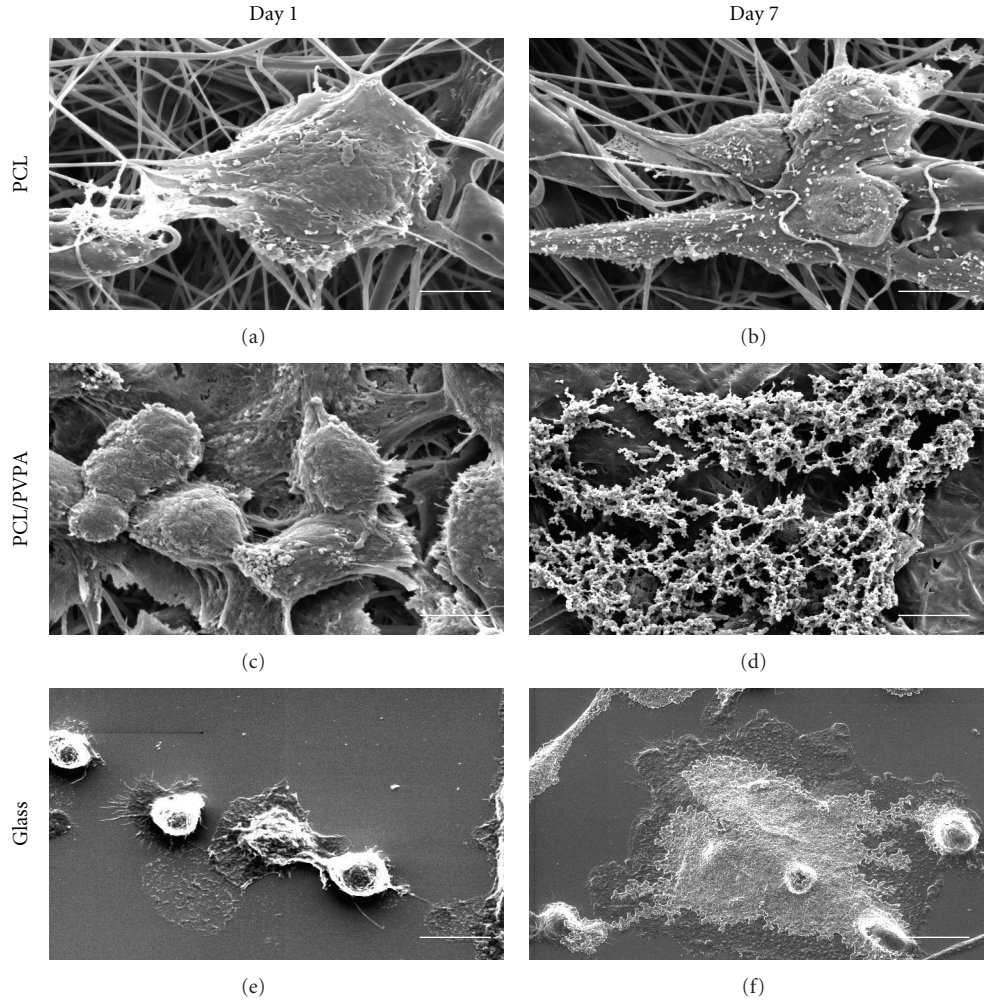

Figure 9: Scanning electron microscope images of osteoclast precursor cells cultured on PCL, PCL/PVPA and glass substrates at day 1 and day 7. PCL and PCL/PVPA, scale bar 5 μm, glass, scale bar 10 μm.

scaffolds displayed superior spreading when compared to the glass substrate. This can be owed to the morphology of the electrospun fibres; the fibrous structure provides a greater surface area for cell attachment, proliferation and integrin binding. At day 7, there was a marked difference in the morphology of cells present on the substrate types. Large, multinucleated cells formed on PCL substrates, which had an elongated, rounded morphology. There were very few cells present on PCL/PVPA substrates; there was evidence of cell debris on the surface. In contrast to cells present on PCL

substrates, cells on the glass surface were multinucleated, however, with a flattened morphology.

It is hypothesised that the presence of PVPA in culture leads to the formation of nonhydrolysable analogues of ATP, AppCp. The accumulation of these analogues within the osteoclast cells leads to loss of its function and eventual cell death [25, 26]. From SEM analysis, it has been shown that cells are present at day 1, suggesting that cells are not apoptosing immediately upon treatment with PVPA.

4. Conclusions

Poly(ε-caprolactone)/poly(vinyl phosphonic acid-co-acrylic acid) (PCL/PVPA) scaffolds have been fabricated using the electrospinning process for use as an active material to enhance bone tissue formation. The concentration of PVPA on the PCL substrate was monitored over 21 days; initially there was a rapid release of PVPA from the PCL substrate, followed by stabilisation of the polymer monolayer. This effect could be advantageous *in vivo* as there would be initial apoptosis of osteoclast cells, providing a greater surface area for osteoblast attachment, proliferation, and subsequent matrix deposition. The attachment of osteoblast cells will be further enhanced due to the hydrophilic nature of the PCL/PVPA scaffold.

The compressive strength of PCL/PVPA has been determined to be an intermediate between cortical bone and trabecular bone, and significantly higher than PCL alone. The strength can be altered depending on the concentration of PVPA. Here we have reported that osteoblast cells are able to attach and proliferate on the PCL/PVPA surface whereas a decrease in osteoclast number is observed. Further studies will be carried out to determine the optimum concentration of PVPA which elicits advantageous materials properties as well as providing the desired biological effects. This study has demonstrated that the PCL/PVPA scaffold has some of the materials properties that are desired in the design of materials for bone tissue engineering.

Acknowledgment

The authors would like to thank The National Institute for Health Research and The Biotechnology and Biological Sciences Research Council for funding the research.

References

[1] R. Langer and J. P. Vacanti, "Tissueengineering," *Science*, vol. 260, no. 5110, pp. 920–926, 1993.

[2] D. Li and Y. Xia, "Electrospinning of nanofibers: reinventing the wheel?" *Advanced Materials*, vol. 16, no. 14, pp. 1151–1170, 2004.

[3] L. L. Hench and J. M. Polak, "Third-generation biomedical materials," *Science*, vol. 295, no. 5557, pp. 1014–1017, 2002.

[4] M. M. Stevens and J. H. George, "Exploring and engineering the cell surface interface," *Science*, vol. 310, no. 5751, pp. 1135–1138, 2005.

[5] C. Li, C. Vepari, H. J. Jina, H. J. Kima, and D. L. Kaplan, "Electrospun silk-BMP-2 scaffolds for bone tissue engineering," *Biomaterials*, vol. 27, no. 16, pp. 3115–3124, 2006.

[6] J. Venugopal, P. Vadgama, T. S. Sampath Kumar, and S. Ramakrishna, "Biocomposite nanofibres and osteoblasts for bone tissue engineering," *Nanotechnology*, vol. 18, no. 5, pp. 55101–55109, 2007.

[7] M. Zakikhani, "United States Patent 5980776," 1999.

[8] A. K. Bassi, J. E. Gough, M. Zakikhani, and S. Downes, "Bone tissue regeneration," in *Electrospinning for Tissue Regeneration*, L. A. Bosworth and S. Downes, Eds., pp. 93–110, Woodhead Publishing, Cambridge, UK, 2011.

[9] R. G. G. Russell and M. J. Rogers, "Bisphosphonates: from the laboratory to the clinic and back again," *Bone*, vol. 25, no. 1, pp. 97–106, 1999.

[10] M. J. Rogers, "New insights into the molecular mechanisms of action of bisphosphonates," *Current Pharmaceutical Design*, vol. 9, no. 32, pp. 2643–2658, 2003.

[11] A. A. Reszka, J. M. Halasy-Nagy, P. J. Masarachia, and G. A. Rodan, "Bisphosphonates act directly on the osteoclast to induce caspase cleavage of Mst1 kinase during apoptosis," *The Journal of Biological Chemistry*, vol. 274, no. 49, pp. 34967–34973, 1999.

[12] C. M. Agrawal and R. B. Ray, "Biodegradable polymeric scaffolds for musculoskeletal tissue engineering," *Journal of Biomedical Materials Research*, vol. 55, no. 2, pp. 141–150, 2001.

[13] D. Puppi, F. Chiellini, A. M. Piras, and E. Chiellini, "Polymeric materials for bone and cartilage repair," *Progress in Polymer Science*, vol. 35, no. 4, pp. 403–440, 2010.

[14] M. P. Lutolf, J. L. Lauer-Fields, H. G. Schmoekel et al., "Synthetic matrix metalloproteinase-sensitive hydrogels for the conduction of tissue regeneration: engineering cell-invasion characteristics," *Proceedings of the National Academy of Sciences of the United States of America*, vol. 100, no. 9, pp. 5413–5418, 2003.

[15] J. Wilson-Hench, "Osteoinduction," in *Progress in Biomedical Engineering*, D. F. Williams, Ed., vol. 4 of *Definitions in Biomaterials*, p. 29, Elsevier, Amsterdam, The Netherlands, 1987.

[16] T. Albrektsson, P. I. Brånemark, H. A. Hansson, and J. Lindström, "Osseointegrated titanium implants. Requirements for ensuring a long-lasting, direct bone-to-implant anchorage in man," *Acta Orthopaedica Scandinavica*, vol. 52, no. 2, pp. 155–170, 1981.

[17] E. Boanini, P. Torricelli, M. Gazzano, R. Giardino, and A. Bigi, "Alendronate-hydroxyapatite nanocomposites and their interaction with osteoclasts and osteoblast-like cells," *Biomaterials*, vol. 29, no. 7, pp. 790–796, 2008.

[18] A. L. Oliveira, A. J. Pedro, C. Saiz Arroyo et al., "Biomimetic Ca-P coatings incorporating bisphosphonates produced on starch-based degradable biomaterials," *Journal of Biomedical Materials Research Part B*, vol. 92, no. 1, pp. 55–67, 2010.

[19] D. Puppi, A. M. Piras, F. Chiellini et al., "Optimized electro- and wet-spinning techniques for the production of polymeric fibrous scaffolds loaded with bisphosphonate and hydroxyapatite," *Journal of Tissue Engineering and Regenerative Medicine*, vol. 5, no. 4, pp. 253–263, 2011.

[20] P. X. Ma, "Biomimetic materials for tissue engineering," *Advanced Drug Delivery Reviews*, vol. 60, no. 2, pp. 184–198, 2008.

[21] H. Zhang and Z. Chen, "Fabrication and characterization of electrospun PLGA/MWNTs/ hydroxyapatite biocomposite scaffolds for bone tissue engineering," *Journal of Bioactive and Compatible Polymers*, vol. 25, no. 3, pp. 241–259, 2010.

[22] J. H. Jang, O. Castano, and H. W. Kim, "Electrospun materials as potential platforms for bone tissue engineering," *Advanced Drug Delivery Reviews*, vol. 61, no. 12, pp. 1065–1083, 2009.

[23] S. H. Kim, H. J. Ha, Y. K. Ko et al., "Correlation of proliferation, morphology and biological responses of fibroblasts on LDPE with different surface wettability," *Journal of Biomaterials Science, Polymer Edition*, vol. 18, no. 5, pp. 609–622, 2007.

[24] E. Sackmann and R. F. Bruinsma, "Cell adhesion as wetting transition?" *European Journal of Chemical Physics and Physical Chemistry*, vol. 12, pp. 262–269, 2002.

[25] J. C. Frith, J. Monkkonen, S. Auriola, H. Monkkonen, and M. J. Rogers, "The molecular mechanism of action of the antiresorptive and anti-inflammatory drug clodronate: evidence for the formation in vivo of a metabolite that inhibits bone resorption and causes osteoclast and macrophage apoptosis," *Arthritis & Rheumatism*, vol. 244, pp. 2201–2210, 2001.

[26] P. P. Lehenkari, M. Kellinsalmi, J. P. Napankangas, K. V. Ylitalo, J. Monkkonen, and M. J. Rogers, "Further insight into mechanism of action of clodronate: inhibition of mitochondrial ADP/ATP translocase by a nonhydrolyzable, adenine-containing metabolite," *Molecular Pharmacology*, vol. 61, no. 5, pp. 1255–1262, 2002.